

Article scientifique

Article

2021

Accepted version

Open Access

This is an author manuscript post-peer-reviewing (accepted version) of the original publication. The layout of the published version may differ .

Determination of the Intracellular Complexation of Inorganic and Methylmercury in Cyanobacterium *Synechocystis* sp. PCC 6803

Garcia Calleja, Javier; Cossart, Thibaut; Pedrero, Zoyne; Santos, João; Ouerdane, Laurent; Tessier, Emmanuel; Slaveykova, Vera; Amouroux, David

How to cite

GARCIA CALLEJA, Javier et al. Determination of the Intracellular Complexation of Inorganic and Methylmercury in Cyanobacterium *Synechocystis* sp. PCC 6803. In: Environmental science & technology, 2021, vol. 55, n° 20, p. 13971–13979. doi: 10.1021/acs.est.1c01732

This publication URL: <https://archive-ouverte.unige.ch/unige:156195>

Publication DOI: [10.1021/acs.est.1c01732](https://doi.org/10.1021/acs.est.1c01732)

Determination of the intracellular complexation of inorganic and methylmercury in cyanobacterium *Synechocystis* sp. PCC 6803.

Javier Garcia-Calleja*¹, Thibaut Cossart², Zoyne Pedrero*¹, João P. Santos², Laurent Ouerdane¹,
Emmanuel Tessier¹, Vera I. Slaveykova², David Amouroux¹

¹ Université de Pau et des Pays de l'Adour, E2S UPPA, CNRS, IPREM, Institut des Sciences Analytiques et de Physico-chimie pour l'Environnement et les matériaux, Pau, France,

² University of Geneva, Faculty of Sciences, Earth and Environment Sciences, Department F.-A. Forel for Environmental and Aquatic Sciences, Uni Carl Vogt, 66 Bvd. Carl Vogt, CH-1211 Geneva, Switzerland

Corresponding Authors:

Javier Garcia-Calleja E-mail: javier.garcia-calleja@univ-pau.fr (J.C) phone: +34 669159412

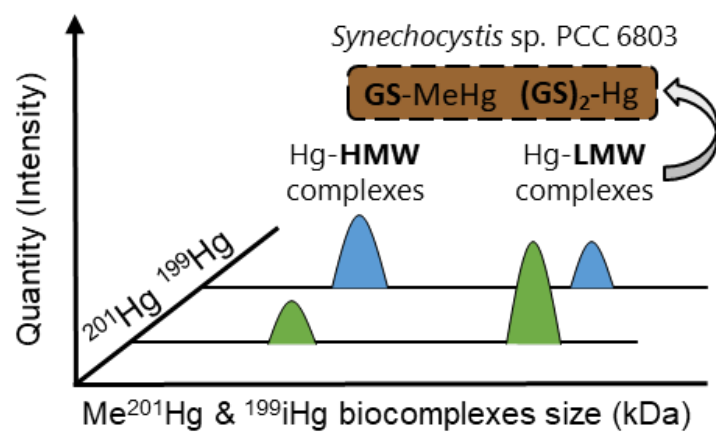
Zoyne Pedrero E-mail: zoyne.pedrerozayas@univ-pau.fr (Z.P) phone: +33 540175027

ABSTRACT.

Understanding of mercury (Hg) complexation with low molecular weight (LMW) bioligands will help elucidate its speciation. In natural waters, the rate of this complexation is governed by physicochemical, geochemical and biochemical parameters. However, the role of bioligands involved in Hg intracellular handling by aquatic microorganisms is not well documented. Here, we combine the use of isotopically-labelled Hg species (inorganic and monomethyl mercury, iHg & MeHg) with hyphenated techniques based on gas or liquid chromatography coupling to elemental and molecular mass spectrometry to explore the role of intracellular biogenic ligands involved in iHg and MeHg speciation in cyanobacterium *Synechocystis* sp. PCC 6803, a representative phytoplankton species. The experiment was carried out at low Hg concentration (3 nM / 600 ng L⁻¹ ¹⁹⁹iHg & 0.3 nM / 60 ng L⁻¹ Me²⁰¹Hg), one of the lowest reported so far for Hg species incubation with photosynthetic unicellular organisms. This approach allowed us to track resulting metabolic and newly-found intracellular Hg biocomplexes (e.g. organic thiols) in *Synechocystis* sp. PCC 6803. In the cytosolic fraction, we found different Hg species binding affinities with both high and low molecular weight (HMW & LMW) bioligands after 5 minutes and 24 hours of Hg exposure in the exponential and stationary phase. Furthermore, the parallel detection with both elemental and molecular ionization sources allowed the sensitive detection and molecular identification of glutathione (GSH) as the main low molecular weight binding ligand to iHg ((GS)₂-Hg) and MeHg (GS-MeHg) in the cytosolic fraction. Such novel experimental approach expands our knowledge on the role of biogenic ligands involved in iHg and MeHg intracellular handling in cyanobacterium.

KEYWORDS: Phytoplankton, cyanobacteria, Hg speciation, LMW thiols, mass spectrometry, glutathione.

39 **Graphical abstract:**



40

41

INTRODUCTION

In recent years, the advanced state-of-the art analytical methodologies for the determination of low molecular weight (LMW) thiols in aquatic system have been developed based on a derivatization step with several reagents to enhance their chemical stability before the analysis¹⁻⁵. Thiols can be separated by liquid chromatography (LC) and detected by fluorescence¹, molecular absorption (ultraviolet/visible detection)⁶ or electrospray ionization (ESI) coupled to tandem mass spectrometry (LC-ESI-MS/MS)². For example, six LMW thiols (mercaptoacetic acid, cysteine, homocysteine, N-acetyl-cysteine, mercaptoethane-sulfonate and glutathione) with concentrations from 7 to 153 nM were determined in a freshwater lake and three boreal wetlands². Also, five LMW thiols (cysteine, thioglycolic acid, N-acetyl-L-cysteine, 3-mercaptopropionic acid and glutathione) were detected ranging from nM to μ M levels in wetland interstitial waters¹. Several LMW thiols were found in benthic biofilm and green algae's periphyton dominated by cysteine and 3-mercaptopropionic acid in the Bolivian Altiplano lakes³. Furthermore, studies focused on biofilms revealed that the extracellular thiols concentration were up to 3 orders of magnitude higher in biofilms than that in the surrounding water suggesting that microorganisms in the biofilm could have a significant impact on Hg bioavailability through the excretion of LMW thiols⁵. The quantification of 6 to 14 LMW thiol compounds with variable concentrations was also achieved in the extracellular medium of anaerobic bacteria, in boreal wetland porewaters and in two coastal sea waters⁴.

Thiols are known to be important ligands for trace metals and known to affect the speciation of several trace metals, such as Ag, Cd, Hg, their bioavailability and transformation in aquatic environment. For example, thiols form complexes with inorganic mercury (iHg) and

monomethylmercury (MeHg) with structures of $\text{Hg}(\text{SR})_2$ or MeHgSR (R-S- being a thiolate organic ligand)⁷. The characterization of resulting Hg-biocomplexes together with their quantification will provide an important information about the role of LMW thiol bioligands involved in Hg speciation and bioavailability. Indeed, freshwater alga *Selenastrum capricornutum* was exposed to MeHg complexed by environmental relevant thiols to study the influence of the chemical structure and thermodynamic stability of MeHg complexes⁸. The complexation of iHg and MeHg with bioligands, such as thiols, could promote several abiotic and biotic transformations such as reduction, methylation or demethylation but also, the iHg and MeHg bioaccumulation^{10–12}. The intracellular bioligands could sequester Hg compounds thus detoxifying mercury and affecting its trophic transfer^{13,14}. Beside our improved knowledge about microbial Hg speciation in environment, the factors that control the intracellular iHg and MeHg speciation and thus toxicity outcome are poorly understood.

Recent advanced state-of-the art analytical methodologies for the determination of low molecular weight (LMW) thiols in aquatic system have been developed based on a derivatization step with several reagents to enhance their chemical stability before the analysis^{1–5}. Thiols can be separated by liquid chromatography (LC) and detected by fluorescence¹, molecular absorption (ultraviolet/visible detection)⁶ or electrospray ionization (ESI) coupled to tandem mass spectrometry (LC-ESI-MS/MS)². For example, six LMW thiols (mercaptoacetic acid, cysteine, homocysteine, N-acetyl-cysteine, mercaptoethane-sulfonate and glutathione) with concentrations from 7 to 153 nM were determined in a freshwater lake and three boreal wetlands². Also, five LMW thiols (cysteine, thioglycolic acid, N-acetyl-L-cysteine, 3-mercaptopropionic acid and glutathione) were detected ranging from nM to μM levels in wetland interstitial waters¹. Several LMW thiols were found in benthic biofilm and green algae's periphyton dominated by cysteine

and 3-mercaptopropionic acid in the Bolivian Altiplano lakes³. Furthermore, studies focused on biofilms revealed that the extracellular thiols concentration were up to 3 orders of magnitude higher in biofilms than that in the surrounding water suggesting that microorganisms in the biofilm could have a significant impact on Hg bioavailability through the excretion of LMW thiols⁵. The quantification of 6 to 14 LMW thiol compounds with variable concentrations was also achieved in the extracellular medium of anaerobic bacteria, in boreal wetland porewaters and in two coastal sea waters⁴. Additionally, a recent novel analytical methodology was developed by optimizing online preconcentration via solid phase extraction (SPE). Achieving detection limits at pM levels and allowing the quantification of several MeHg-thiol complexes in the extracellular fraction of the bacterium *Geobacter sulfurreducens* PCA previously exposed to 100 nM of iHg⁹.

However, the determination of Hg-biocomplexes in phytoplankton at environmental realistic concentration has not been reported yet in aquatic system and need to be fulfilled for a better understanding of the role of bioligands in Hg speciation.

Hyphenated techniques based on liquid chromatography coupled to inductively coupled plasma mass spectrometry (ICP-MS) and/or molecular mass spectrometry have been implemented to look into the wide spectrum at low and high molecular weight (HMW) Hg biocomplexes¹⁵. Particularly, the use of hydrophilic interaction liquid chromatography (HILIC) coupled in parallel detection with ICP-MS and ESI-MS/MS have been used to identify the structural characterization of several metal-complexes in different biological matrices. For example, the identification of Hg bound to several biothiols in plants¹⁶, the characterization of Hg-metallothioneins complexes in dolphin liver¹⁷ and selenium metabolites in human urine and blood¹⁸ among others¹⁹. A recent study using high-resolution mass spectrometry revealed that the molecular composition of Hg binding dissolved organic matter (DOM) released by green algae *Chlorella vulgaris*, *Chlamydomonas*

110 *reinhardtii* and *Scenedesmus obliquus* depended on natural variation in light intensity and other
111 physicochemical parameters²⁰.

112 Isotopically labelled Hg species were employed for the identification of iHg and MeHg binding
113 affinities to biomolecules in living aquatic organisms²¹. But also, their localization in different cell
114 compartments in methylating and non-methylating sulfate reducing bacteria was achieved¹⁵. In this
115 previous work, the combination of Hg enriched isotopes with gaseous chromatography (GC)/LC-
116 ICP-MS demonstrated that HMW bioligands released from a methylating strain were exclusively
117 bound to MeHg, however, no structural characterization was provided. The identification of Hg
118 binding HMW proteins requires several purification steps in order to characterize the target
119 protein²².

120 The existing literature of Hg biocomplexes characterization in aquatic microorganisms is limited
121 in terms of molecular mass spectrometry characterization. Using X-ray absorption spectroscopy
122 high energy resolution fluorescence detected X ray absorption near edge structure (XAS-HERFD-
123 XANES or HR-XANES), several Hg species were identified inside biological cells²³⁻²⁵. But also,
124 X-ray absorption spectroscopy fine structure (EXAFS) can be used to elucidate the structural
125 characterization of thiol functional groups among others (O/N) binding iHg^{26,27}.

126 In this work, the study of intracellular complexation of Hg species was carried out by taking
127 advantage of the tracking with isotopically enriched isotopes. The enriched isotopic tracers (¹⁹⁹iHg
128 and Me²⁰¹Hg) were added after cells resuspension in the exposure medium with the purpose of
129 tracing the newly formed Hg biocomplexes in the cytosolic fraction. The main aim of this research
130 was to characterize Hg-biocomplexes involved in Hg speciation and to study different Hg species
131 specific binding affinities at two different growth phases in the intracellular fraction of the

cyanobacterium *Synechocystis* sp. PCC 6803. This model cyanobacterium is representative from freshwater ecosystems, a prokaryotic cell with a single chromosome free in cytoplasm and capable of growth by oxygenic photosynthesis or by glycolysis and oxidative phosphorylation in dark conditions; a phytoplankton microorganism structurally and metabolically more similar to bacteria than an eukaryotic cell that can be found in microbial and phytoplankton communities^{28,29}. Then, the combination of complementary information obtained by hyphenated analytical techniques such as GC-ICP-MS, size exclusion chromatography (SEC) -ICP-MS and HILIC-ICP/ESI-MS provide new insights on the role of intracellular ligands in Hg speciation and intracellular fate in photosynthetic microorganisms.

MATERIAL AND METHODS.

Reagent and Standards. All solutions were prepared using ultrapure water (18 MΩ cm, Millipore). All samples and standards were prepared with trace metal grade acid (Fisher Scientific Illkrich, France). Working standard solutions were prepared daily by appropriate dilution of the stock standard solutions in 1% of hydrochloric acid (HCl) and stored at 4 °C until use. ¹⁹⁹Hg-enriched inorganic mercury and ²⁰¹Hg-enriched methylmercury (ISC-Science, Oviedo, Spain) were used as incubation spikes or tracers. ¹⁹⁸Hg-enriched inorganic mercury and ²⁰²Hg-enriched methylmercury were used to quantify the endogenous Hg species (¹⁹⁹iHg and Me²⁰¹Hg) present in the bulk and cytosolic fraction. Hg species were derivatized by using sodium tetraethyl borate (NaBEt₄, Merseburger spezial Chemikalien, Germany). Glutathione standard was purchased from Sigma Aldrich (Saint-Quentin-Fallavier, France). The rabbit liver metallothionein-2 isoform standard was purchased from Enzo life sciences (Villeurbanne, France). Sample flasks were cleaned using three successive baths comprising an ultrasonicator bath during 1 hour in nitric acid (HNO₃) 10% (v/v) (twice) and HCl 10% (v/v) (once).

Experimental procedure.

Culture conditions: *Synechocystis* sp. PCC 6803 was purchased from the Pasteur Culture collection of Cyanobacteria (PCC, <https://research.pasteur.fr/en/team/collection-of-cyanobacteria/>) and cultivated using modified BG11 medium (sodium nitrate replaced by ammonium nitrate) with illumination values of 130 μE m⁻² s⁻¹ and illumination regime of 14:10 h (light : dark)³⁰

Sampling procedure: Cells coming from two different cultures in mid-exponential and stationary growth phases were harvested by centrifugation (1300 g, 15 min, 10 °C). At the exponential phase,

the cyanobacterial growth is not limited having a maximal number of growing cells. Contrary, the stationary phase corresponds to a situation in which growth rate and death rate are equal. The number of new cells created is limited by the growth factor and as a result, the rate of cell growth matches the rate of cell death. Under such cellular stress conditions, it has been suggested that specific genetic response are occurring and that the release of extracellular bioligands could be enhanced^{31,32}.

Cells were resuspended in 400 mL of exposure medium (composition in Table S1) to a final cell density (2×10^7 cell mL⁻¹) determined by flow cytometry (Accuri C6, BD Biosciences, Switzerland). Then, 200 mL were used as biotic control to check any possible Hg spike contamination and to measure the Hg background already found in the biological system (Figure S1), while the other 200 mL were spiked with 600 ng and 60 ng of ¹⁹⁹HgCl₂ and Me²⁰¹HgOH per L of exposure media, respectively (3 nM ¹⁹⁹iHg & 0.3 nM Me²⁰¹Hg). An aliquot of 45 mL sample was taken and centrifuged (1300 g, 15 min, 10 °C) at exposure times of 5 min and 24h. Pellets were collected and cells were fractionated to membrane fraction and cytosolic fraction as described below. Three independent cell cultures were carried out and incubated simultaneously with enriched Hg isotopes. The medium was sterile and no contamination occurred with other organisms.

Cell fractionation. Each pellet aliquot was flash frozen in liquid nitrogen to stop the metabolic activity; subsequently 1.5 mL of Milli-Q water was added to the pellet. An Ultra-Sonicator (Sonics Vibra-cell, 130 W, 20 kHz) step was used for 1 minute at 50% amplitude in order to break the cells. Allowing, through a centrifugation (10000 g, 6 min) in a centrifuge 5417R (Eppendorf), the separation of cytosolic fraction (composed by organelles, heat stable proteins (HSP) and heat denatured proteins (HDP)) and membranes with cells debris³³. Cytosolic fraction samples were

divided in aliquots and stored at -80 °C to avoid any possible protein degradation for Hg bioligands analysis. The others were acidified with 3N HNO₃ and stored at 4 °C for the quantification of Hg species. The scheme of the cell fractionation procedure performed for Hg species quantification and the investigation of Hg biocomplexes is displayed in Figure S2.

Analysis of Hg binding biomolecules by SEC/HILIC-ICP-MS and HILIC-ESI-MS.

Instrumentation. An Agilent 1100 liquid chromatography (Agilent, Wilmington, DE) equipped with a binary HPLC pump, an autosampler, and a diode array detector was used. Also, chromatographic separations were carried out using an Agilent 1100 capillary μ HPLC system (Agilent, Tokyo, Japan). An Agilent inductively coupled plasma mass spectrometer (ICP-MS) 7500 ce (Yokogawa Analytical Systems, Tokyo, Japan) served for Hg detection and other metals (Fe, Co, Cu and Zn among others) after liquid chromatography separation. This separation system was also coupled to a linear trap quadrupole (LTQ) Orbitrap Velos mass Spectrometer (Thermo Fisher Scientific, Bremen, Germany) in parallel by means of a heated electrospray ionization source (H ESI II).

Chromatographic separation (SEC and HILIC) conditions. Hg binding biomolecules from cytosolic fraction were separated in the SuperdexTM 200 HR (10 x 300mm x 13 μ m) (Cytiva life sciences) with an operation range of 10 to 600 kDa and used for a wide screening of such biomolecules. For the analysis of LMW compounds, an aliquot from the cytosol (15 μ L) was diluted with acetonitrile (1:2 v/v) in order to precipitate high molecular weight biomolecules following this procedure^{18,22}, with a subsequent addition of 250 μ g of natural inorganic and methylated Hg per L before the injection in a TSKgel[®] amide 80 column (Sigma Aldrich). The hydrophilic interaction liquid chromatography has the advantage of using a polar mobile phase,

being compatible with electrospray ionization and enabling the parallel detection in both analytical instruments. The operating parameters for size exclusion chromatography and hydrophilic interaction liquid chromatography coupled to ICP-MS and ESI-MS analysis are shown in Table **S1**.

To accurately determine the molecular mass range that Hg binding LWM bioligands could be found in the cytosolic fraction (under 16 kDa), a screening was carried out in a SuperdexTM Peptide (Cytiva life sciences) with a separation range between 7 and 0.1 kDa; noticing a match around 0.3 kDa fraction with a standard of glutathione (GSH) injected with the same chromatographic settings (Figure **S3**).

We have also examined LMW bioligands binding iHg and MeHg in the extracellular medium. However, the limitations of the experimental setup and the analytical approach did not allow us to detect any bioligand binding Hg by SEC-ICPMS in the extracellular medium even after 24 hours of Hg exposure.

Hg species quantification.

Instrumentation. A Thermo Electron GC (Trace) coupled to a Thermo Electron ICP-MS (X7 X series) was used for the determination of total concentration of each Hg species.

Sample preparation. The bulk and cytosolic fraction were digested with 3N HNO₃ under an analytical microwave (Discover and Explorer SP-D 80 system, CEM, NC USA) and analyzed by gas chromatography coupled to inductively coupled plasma mass spectrometry (GC-ICP-MS) as detailed elsewhere³⁴. Before starting the analytical procedure, a certain amount of both enriched spikes in ¹⁹⁸iHg and Me²⁰²Hg, previously characterized in terms of isotopic abundances and concentration, were added to the vial containing the sample. After, 5 mL of an acetic acid/acetate buffer (0.1 M, pH 3.9) were aggregated with a pH adjustment to 3.9. Subsequently, Hg species

(endogenous and exogenous) were ethylated using NaBrEt₄ (5% v/v) and extracted in isooctane by automatic shaking for 20 minutes on elliptic table. Quantification of isotopically enriched ¹⁹⁹iHg and Me²⁰¹Hg was carried out by applying isotope pattern deconvolution.

Analytical procedure. The measurement of the isotopic composition of Hg enriched isotopes in the samples was carried out by GC-ICP-MS. Integration of the chromatographic peaks was carried out using the commercial software Thermo Plasma Lab. The methodological detection limit for iHg and MeHg were 0.05 and 0.03 ng L⁻¹ respectively. All operating parameters for the GC-ICP-MS analysis are found in Table S2. Details of the mathematical approach for quantification of the samples by double-double isotope dilution analysis are observed in Figure S4.

RESULTS and DISCUSSION.

Hg species concentration in the cytosolic fraction.

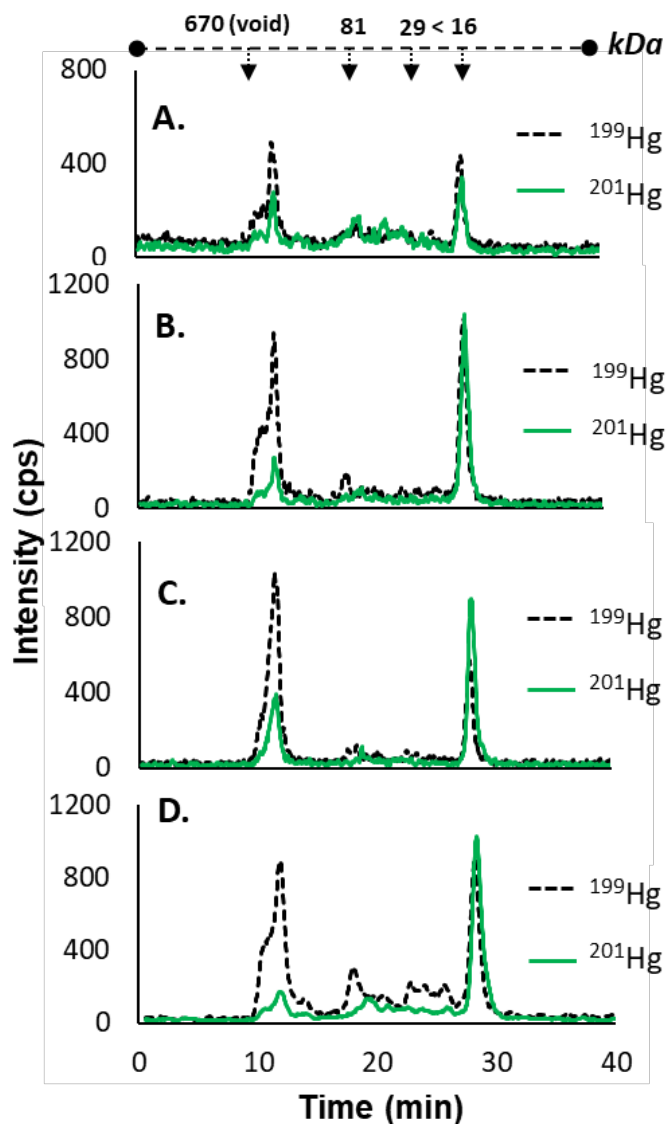
The concentration of ¹⁹⁹iHg and Me²⁰¹Hg in the bulk (exposure medium and cells) and cytosolic fraction of *Synechosystis* sp. PCC 6803 are presented in Table 1. Overall, similar Hg distribution was observed in exponential and stationary phase. The proportion of ¹⁹⁹iHg and Me²⁰¹Hg in the cytosolic fraction ranged between 9-10 % and 32-36 % respectively after 24 hours of Hg exposure at both growth phases. At the beginning (t=5min), the concentration of ¹⁹⁹iHg ranged between 6-8 ng L⁻¹ whereas, for Me²⁰¹Hg ranged between 13-19 ng L⁻¹ in the cytosolic fraction. No large distinctions were found for Me²⁰¹Hg after 24 hours whereas, a higher uptake of ¹⁹⁹iHg was observed at both growth phases.

Table 1. ^{199}iHg and Me^{201}Hg species proportion and concentration (ng L^{-1}) in the bulk (exposure medium and cells) and cytosolic fraction in the beginning (5min) and after 24h exposure of *Synechocystis* sp. PCC 6803 in exponential and stationary growth phases. Mean \pm sd (n=3).

<i>Exponential phase</i>	^{199}iHg		Me^{201}Hg	
	$t_{5\text{min}}$	$t_{24\text{h}}$	$t_{5\text{min}}$	$t_{24\text{h}}$
Bulk (ng L^{-1})	517 ± 14	379 ± 24	52 ± 1	47 ± 3
Cytosolic fraction (ng L^{-1})	6 ± 1	35 ± 9	13 ± 1	15 ± 2
Cytosolic fraction vs Bulk (%)	1.2 ± 0.2	9.2 ± 2.4	25 ± 2	32 ± 4

<i>Stationary phase</i>	^{199}iHg		Me^{201}Hg	
	$t_{5\text{min}}$	$t_{24\text{h}}$	$t_{5\text{min}}$	$t_{24\text{h}}$
Bulk (ng L^{-1})	549 ± 28	421 ± 23	54 ± 1	50 ± 1
Cytosolic fraction (ng L^{-1})	8 ± 3	41 ± 7	19 ± 1	18 ± 1
Cytosolic fraction vs Bulk (%)	1.5 ± 0.5	9.7 ± 1.7	35 ± 2	36 ± 2

265 **Hg binding bioligands screening in the cytosolic fraction.**



266
267 **Figure 1.** Size exclusion chromatograms (Superdex 200 (Range: 600 - 10 kDa)) in the cytosolic fraction of
268 *Synechocystis* sp. PCC 6803 by ICP-MS detection of (A) ^{199}Hg and ^{201}Hg corresponding to both Hg isotopic
269 tracers (^{199}iHg and Me^{201}Hg) after 5 minutes of exposure in the exponential phase. (B) ^{199}Hg and ^{201}Hg
270 corresponding to both isotopic tracers (^{199}iHg and Me^{201}Hg) after 24 hours of exposure in the exponential
271 phase. (C) ^{199}Hg and ^{201}Hg corresponding to both Hg isotopic tracers (^{199}iHg and Me^{201}Hg) after 5 minutes
272 of exposure in the stationary phase. (D) ^{199}Hg and ^{201}Hg corresponding to both isotopic tracers (^{199}iHg and
273 Me^{201}Hg) after 24 hours of exposure in the stationary phase.

274

275 The analysis by SEC-ICP-MS of the cytosolic fraction reveals two main Hg-containing fractions
 276 with HMW (≥ 600 kDa, 10-13 min) and LMW (≤ 16 kDa, 27-29 min) in a range from 600 to 10
 277 kDa (Figure 1). The increase of ^{199}Hg signal was correlated with the exposure time from 5 min to
 278 24h. ^{199}iHg was preferentially bound to HMW biomolecules eluting around 10-13 min at the
 279 beginning of the Hg exposure. After 24 hours, the intensity of ^{199}iHg binding HMW fraction (≥ 600
 280 kDa) remained constant whereas, a remarkable increase in ^{199}Hg intensity was seen at longer
 281 elution time corresponding to fractions of lower molecular weight; from 29 to 81 kDa (17-26 min)
 282 and under 16 kDa (27-29 min). On the other hand, Me^{201}Hg was mostly bound to LMW fraction
 283 exhibiting an intensity increase after 24h exposure at both growth phases.

284 Despite SEC-ICP-MS analysis does not give quantitative information, we have estimated the
 285 proportion of ^{199}iHg and Me^{201}Hg bound to LMW cytosolic ligands (Table 2) based on the peak
 286 area of eluted compounds (Figure 1).

287

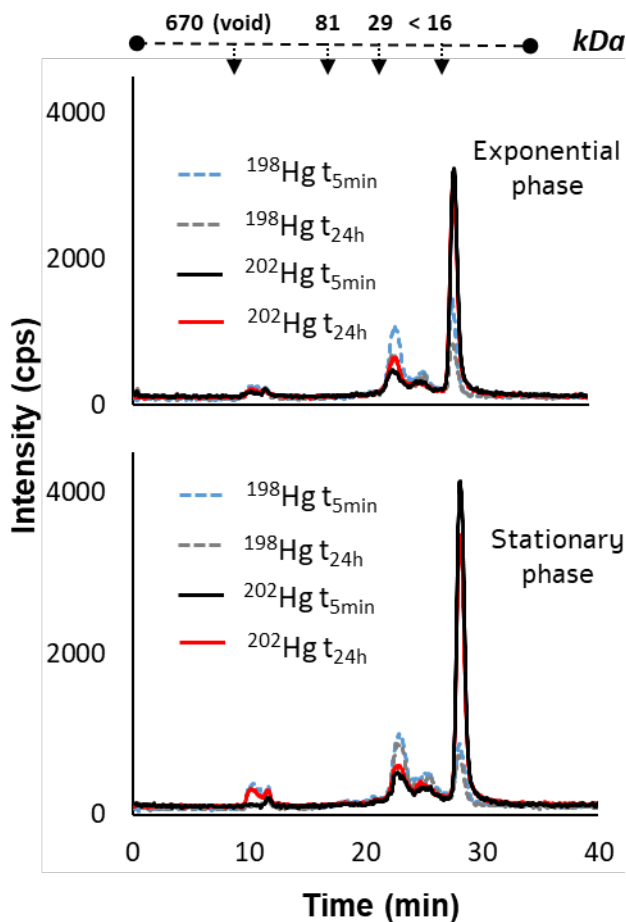
288 **Table 2.** Percentage of ^{199}iHg and Me^{201}Hg bound to LMW fraction of cytosolic ligands at the beginning
 289 and after 24h exposure at different growth phases in *Synechocystis* sp. PCC 6803. Mean \pm sd (n=3).

% Hg binding LMW fraction	^{199}iHg		Me^{201}Hg	
	$t_{5\text{min}}$	$t_{24\text{h}}$	$t_{5\text{min}}$	$t_{24\text{h}}$
Exponential phase	$38 \pm 8 \%$	$47 \pm 11 \%$	$68 \pm 5\%$	$79 \pm 4\%$
Stationary phase	$35 \pm 14 \%$	$46 \pm 8 \%$	$67 \pm 4\%$	$86 \pm 9 \%$

290

291 Table 2 shows the percentage of Hg bound to the LMW fraction at the beginning and after 24
 292 hours of Hg exposure at different growth phases in which the proportion of ^{199}iHg and Me^{201}Hg
 293 bound to the LMW fraction after 24 hours of Hg exposure were 46-47 % and 79-86 % respectively,
 294 at both growth phases.

295 To obtain further information about the specificity and affinity of Hg to bioligands, two different
 296 enriched Hg species (^{198}iHg and Me^{202}Hg) were subsequently added to the cytosolic fraction that
 297 had been previously exposed to ^{199}iHg and Me^{201}Hg (Figure 2).



298
 299 **Figure 2.** Size exclusion chromatograms (Superdex 200 (Range: 600-10 KDa)) in the cytosolic fraction of
 300 *Synechocystis* sp. PCC 6803 in the exponential and stationary growth phase by ICP-MS detection of ^{198}Hg
 301 and ^{202}Hg corresponding to the addition ($5 \mu\text{g L}^{-1}$) of ^{198}iHg and Me^{202}Hg after 5 minutes and 24 hours of
 302 Hg exposure of both isotopic tracers (^{199}iHg and Me^{201}Hg).
 303

304 The obtained results in figure 2 evidenced similar patterns to endogenous Hg biocomplexes
 305 distribution from figure 1 confirming the specific affinity of LMW fraction (27-29 min) for MeHg.

306 But also, it demonstrates that bioligands functional groups in the LMW fraction are still available
307 to bind iHg and MeHg.

308 Overall, the transition from exponential to stationary growth phase involves several adaptations
309 such as changes in proteins expression involved in cell growth, protein biosynthesis involved in
310 nutrient uptake and proteins related to energy metabolism^{32,35}. Nutrient availability is the main
311 critical factor that determines the growth phase changes. In the existing literature, no studies have
312 ever reported comparisons in the distribution of iHg or MeHg binding intracellular ligands between
313 exponential and stationary phase in phytoplankton. Under our experimental conditions, the
314 differences in Hg exposure time or growth phase have not affected the distribution of potential
315 bioligands capable of binding exogenous Hg. This result is important to highlight since the amount
316 of the extracellular ligands released at the stationary phase could be higher³¹ and was expected to
317 influence the amount of the bioaccumulated iHg or MeHg.

318 Understanding of iHg and MeHg intracellular fate is a key factor to explain the role of the
319 intracellular bioligands in Hg speciation. In our work, the increase of the signal intensity of ¹⁹⁹iHg
320 and Me²⁰¹Hg bound to the LMW fraction (< 16 kDa) after 24 h in the stationary phase suggests
321 that these specific biomolecules, where heat stable proteins among others are present, could be
322 involved in Hg species specific sequestration at nontoxic levels. This falls in agreement with recent
323 observations of the synthesis of glutathione and PCs by a marine diatom *Thalassiosira weissflogii*
324 when exposed to iHg and MeHg^{36,37}. Furthermore, the findings concerning the species specific
325 affinity of iHg binding HMW fraction and MeHg binding LMW fraction agree with a previous
326 study carried out with three marine phytoplankton (*Thalassiosira pseudonana*, *Chlorella*
327 *autotrophica* and *Isochrysis galbana*), where heat stable proteins were mainly binding MeHg
328 whereas iHg was associated to the organelles fraction³⁸. However, these experiments are not

directly comparable since higher Hg concentrations were added in comparison with our work (> 150 folds for iHg).

Although the specific function of these biogenic intracellular ligands cannot be clarified with the available data, the Hg binding bioligands detected may also be involved in several Hg transformations such as biotic reduction or biotic demethylation^{39,40}. It should be noticed that so far only two studies reported the use of simultaneous enriched isotopes for iHg and MeHg in cell culture experiments. On one hand, to investigate the Hg species accumulation and biotic transformations in *C. reinhardtii*³⁹ and on the other hand, to explore the Hg biocomplexes distribution size in the extracellular and intracellular fraction in methylating and non methylating sulfate-reducing bacteria¹⁵. Nevertheless, no structural characterization of Hg biocomplexes was provided. Additionally, most of the studies focused on the intracellular compartment of phytoplankton cell cultures have been carried out under high Hg exposure concentrations (1000-10000 higher than our conditions), in order to study the Hg accumulation, subcellular distribution and detoxification mechanisms³⁸⁻⁴². On the contrary, our work used lower Hg concentrations of 3 nM / 600 ng L⁻¹ for ¹⁹⁹iHg and 0.3 nM / 60 ng L⁻¹ for Me²⁰¹Hg. Therefore, it is not expected to have induced considerable physiological changes in the main intracellular processes^{43,44}. Additionally, other essential elements (Cu, Zn, Fe and Co) were monitored by SEC-ICP-MS. In this case, Hg exposure compared with the biotic controls (no Hg exposure) did not induce the formation of new metal-biocomplexes fractions in their SEC chromatogram profiles (Figure S5).

Identification of intracellular Hg species-specific biogenic complexes in the low molecular weight fraction.

The identification of biomolecules is usually based on the retention time matching of standards and samples. However, the structural characterization provides an unambiguous identification of the molecular structure, representing a step further in terms of Hg biocomplexes determination.

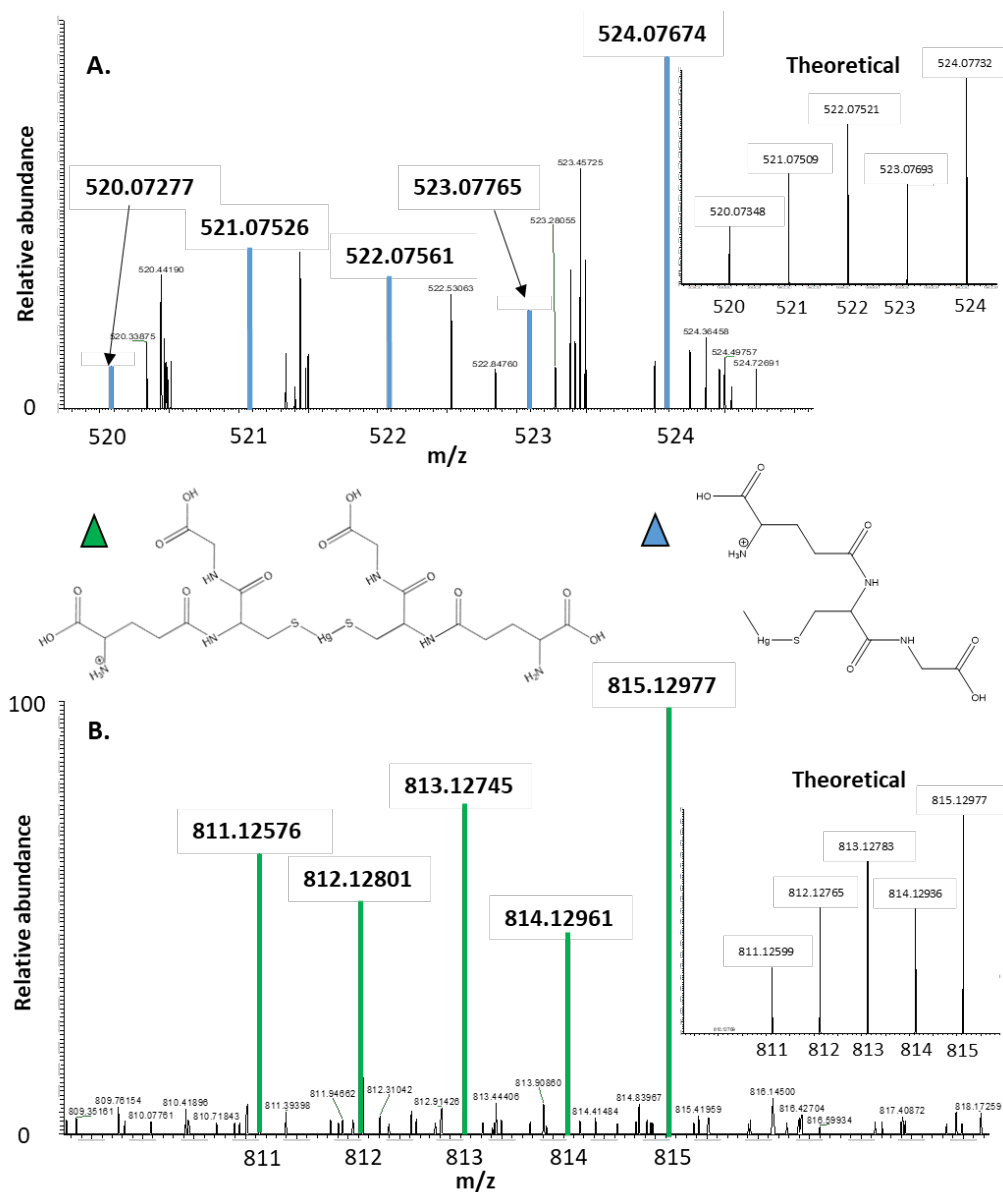


Figure 3. (A) Zoom of the mass spectra obtained at 21.2 min demonstrates the presence of MeHg binding one glutathione with its natural Hg isotopic pattern (^{202}Hg m/z = 524.08). (B). Zoom of the mass spectra obtained at 23.5 min demonstrate the presence of Hg binding two glutathione with its natural Hg isotopic pattern in stationary phase (^{202}Hg m/z = 815.13).

359

360 The analysis by HILIC-ICP-MS of the cytosolic fraction reveals two Hg binding bioligands
361 corresponding to two different peaks with specific retention times at 21.0 min and 23.7 min (Figure
362 S6A) based on Hg isotopes monitoring (elemental ionization). For this purpose, the injection of
363 the same cytosolic fraction carrying out the same chromatographic settings (leading to matching
364 retention times) was done by coupling to an electrospray ionization mass spectrometer and
365 providing structural information about the compounds previously detected (Figure S6B). Firstly,
366 the natural isotopic pattern of Hg was investigated in the full scan spectra at both retention times.
367 Electrospray MS at the retention time of first peak revealed one ion with the isotopic pattern of
368 mercury (Figure 3A) at $m/z = 524.08$ (m/z corresponding to the most abundant isotope in the
369 isotopic distribution). This mass to charge ratio corresponded to Hg methylated binding one
370 glutathione (GS-MeHg, $C_{11}H_{20}HgN_3O_6S^+$). Regarding the second peak, the Hg isotopic pattern
371 was observed (Figure 3B) at $m/z = 815.13$ corresponding to iHg binding two glutathione ((GS)₂-
372 Hg), $C_{20}H_{33}HgN_6O_{12}S_2^+$). Even if the theoretical natural isotopic pattern for iHg and MeHg
373 binding glutathione did not match in all isotopes in comparison with the experimental Hg isotopic
374 patterns, caused by the low concentration of iHg and MeHg bound to GSH, the experimental
375 masses agreed with the theoretical ones.

376 The present results confirmed that GSH is playing a key role in Hg sequestration in different
377 aquatic microorganisms^{37,45}. Particularly in cyanobacteria, GSH plays a central role in redox
378 control of protein thiols and disulfide bonds, including protection against toxic metabolites,
379 xenobiotic and oxidative stress^{46,47}. Hg exposure is well known to induce accumulation of reactive
380 oxygen species and peroxidation products in phytoplankton⁴³. Under oxidative stress, glutathione
381 acts as a protein reductant against highly reactive oxidants such as singlet oxygen, superoxide and

hydroxyl radicals forming GS-SG²⁹. Nevertheless, the reduction of GS-SG (S-S) to two GSH is mediated by the enzyme glutathione reductase being a critical process for its regeneration. Exposure of green alga *Chlamydomonas reinhardtii* to sub-toxic concentrations of iHg and MeHg resulted in a significant increase of reduced glutathione after Hg-treatments⁴⁴. GSH is a precursor of phytochelatins synthesis, which can be activated following the exposure to different toxic metals including Hg⁴⁴. The cyanobacterial phytochelatin synthesis was shown to be close functionally to that of plants. Additionally, the phytochelatin synthase exhibited transpeptidasic activity during Cd- exposure, being able to synthesize phytochelatins with a degree of oligomerization higher than PC₂⁴⁸. Furthermore, Hg exposure induced changes in intracellular thiols concentration such as glutathione or phytochelatins demonstrating that algae can control the intracellular Hg speciation^{36,37,40}. Phytoplankton intracellular detoxification mechanisms can promote the transformation of iHg into gaseous Hg^{37,49}. In bacteria, it was shown that the intracellular reduction is carried out enzymatically⁵⁰.

In the extracellular fraction, several studies have demonstrated the influence of LMW bioligands on Hg speciation^{51,52}. Particularly, high rates of iHg uptake and biotic methylation were observed in the presence of some complexing LMW thiols such as cysteine whereas, GSH inhibited these processes⁵². These results suggest that the molecular structure of the bioligands plays a crucial role in Hg speciation in anaerobic environments. Additional information was obtained in a freshwater green microalga *Selenastrum capricornutum*⁸. Skrobonja et al. 2019 showed that the thermodynamic stability in turns with the chemical structure of MeHg LMW complexes in the extracellular medium govern the rate of MeHg interactions with the cell surface⁸. Further investigations must be carried out to explore the role of these intra- and extra-cellular ligands in

Hg speciation but also, structural studies based on molecular mass spectrometry will be needed to elucidate the exact function of the biomolecules involved in Hg speciation.

Environmental perspective

The identification of glutathione as a bioligand binding to iHg ((GS)₂-Hg) and MeHg (GS-MeHg) in cyanobacterium *Synechocystis* sp. PCC 6803 has demonstrated that glutathione plays an important role in Hg intracellular handling; reducing probably the potential damage that both Hg species could cause on the cellular metabolism. In aquatic environment, cyanobacteria are found in various environmental settings interacting with different aquatic microorganisms with a specific role into the natural Hg cycle. The pioneering approach based on the combination of enriched isotopes and mass spectrometry techniques represent a first step, towards explaining and understanding the intracellular speciation of iHg and MeHg in photosynthetic microorganisms. Important emphasis should be placed concerning to global warming and/or water pollution⁵³. Particularly, cyanobacteria are considered to prevail in warmer freshwaters and their proportion will increase in phytoplankton communities⁵⁴. Cyanobacteria are more resistant to pollutant exposure, high temperatures and eutrophication events caused by the global warming or nutrient contamination than other phytoplankton species^{55,56}. Furthermore, phytoplankton communities are the main entry point in the trophic transfer for Hg. For these reasons, our results exemplify the potential bioaccumulation of iHg and MeHg at nontoxic levels by a model phytoplankton.

Notes

The authors declare no competing financial interest.

ACKNOWLEDGMENTS

Financial support from Agence National de la Recherche (ARN) (Project-ANR-17-CE34-0014) and Swiss National Science Foundation (SNF) (project N 175721) in the framework of the PHYTAMBA project (PRCI ANR/SNSF). Financial support from E2S/UPPA (Energy and Environment Solutions) in the framework of the MESMIC Hub (Metals in Environmental System Microbiology).

REFERENCES

- (1) Zhang, J.; Wang, F.; House, J. D.; Page, B. Thiols in Wetland Interstitial Waters and Their Role in Mercury and Methylmercury Speciation. *Limnology and Oceanography* **2004**, *49* (6), 2276–2286. <https://doi.org/10.4319/lo.2004.49.6.2276>.
- (2) Liem-Nguyen, V.; Bouchet, S.; Björn, E. Determination of Sub-Nanomolar Levels of Low Molecular Mass Thiols in Natural Waters by Liquid Chromatography Tandem Mass Spectrometry after Derivatization with p-(Hydroxymercuri) Benzoate and Online Preconcentration. *Anal. Chem.* **2015**, *87* (2), 1089–1096. <https://doi.org/10.1021/ac503679y>.
- (3) Bouchet, S.; Goñi-Urriza, M.; Monperrus, M.; Guyoneaud, R.; Fernandez, P.; Heredia, C.; Tessier, E.; Gassie, C.; Point, D.; Guédron, S.; Achá, D.; Amouroux, D. Linking Microbial Activities and Low-Molecular-Weight Thiols to Hg Methylation in Biofilms and Periphyton from High-Altitude Tropical Lakes in the Bolivian Altiplano. *Environmental Science & Technology* **2018**, *52* (17), 9758–9767. <https://doi.org/10.1021/acs.est.8b01885>.
- (4) Liem-Nguyen, V.; Huynh, K.; Gallampois, C.; Björn, E. Determination of Picomolar Concentrations of Thiol Compounds in Natural Waters and Biological Samples by Tandem Mass Spectrometry with Online Preconcentration and Isotope-Labeling Derivatization. *Analytica Chimica Acta* **2019**, *1067*, 71–78. <https://doi.org/10.1016/j.aca.2019.03.035>.
- (5) Leclerc, M.; Planas, D.; Amyot, M. Relationship between Extracellular Low-Molecular-Weight Thiols and Mercury Species in Natural Lake Periphytic Biofilms. *Environmental Science & Technology* **2015**, *49* (13), 7709–7716. <https://doi.org/10.1021/es505952x>.
- (6) Kuśmierk, K.; Chwatko, G.; Głowacki, R.; Kubalczyk, P.; Bald, E. Ultraviolet Derivatization of Low-Molecular-Mass Thiols for High Performance Liquid Chromatography and Capillary Electrophoresis Analysis. *Journal of Chromatography B* **2011**, *879* (17–18), 1290–1307. <https://doi.org/10.1016/j.jchromb.2010.10.035>.
- (7) G. Berthon. The Stability Constants of Metal Complexes of Amino Acids with Polar Side Chains. *Pure & Appl. Chem.* **1995**, *69*, 1117–1240. <https://doi.org/10.1351/PAC199567071117>.
- (8) Skrobonja, A.; Gojkovic, Z.; Soerensen, A. L.; Westlund, P.-O.; Funk, C.; Björn, E. Uptake Kinetics of Methylmercury in a Freshwater Alga Exposed to Methylmercury Complexes with Environmentally Relevant Thiols. *Environ. Sci. Technol.* **2019**, *acs.est.9b05164*. <https://doi.org/10.1021/acs.est.9b05164>.

- (9) Liem-Nguyen, V.; Nguyen-Ngoc, H.-T.; Adediran, G. A.; Björn, E. Determination of Picomolar Levels of Methylmercury Complexes with Low Molecular Mass Thiols by Liquid Chromatography Tandem Mass Spectrometry and Online Preconcentration. *Anal Bioanal Chem* **2020**. <https://doi.org/10.1007/s00216-020-02389-y>.
- (10) Monperrus, M.; Tessier, E.; Amouroux, D.; Leynaert, A.; Huonnic, P.; Donard, O. F. X. Mercury Methylation, Demethylation and Reduction Rates in Coastal and Marine Surface Waters of the Mediterranean Sea. *Marine Chemistry* **2007**, *107* (1), 49–63. <https://doi.org/10.1016/j.marchem.2007.01.018>.
- (11) Lalonde, J. D.; Amyot, M.; Kraepiel, A. M. L.; Morel, F. M. M. Photooxidation of Hg(0) in Artificial and Natural Waters. *Environmental Science & Technology* **2001**, *35* (7), 1367–1372. <https://doi.org/10.1021/es001408z>.
- (12) Celo, V.; Lean, D. R. S.; Scott, S. L. Abiotic Methylation of Mercury in the Aquatic Environment. *Science of The Total Environment* **2006**, *368* (1), 126–137. <https://doi.org/10.1016/j.scitotenv.2005.09.043>.
- (13) Grégoire, D. S.; Poulain, A. J. A Little Bit of Light Goes a Long Way: The Role of Phototrophs on Mercury Cycling. *Metallomics* **2014**, *6* (3), 396. <https://doi.org/10.1039/c3mt00312d>.
- (14) Le Faucheur, S.; Campbell, P. G. C.; Fortin, C.; Slaveykova, V. I. Interactions between Mercury and Phytoplankton: Speciation, Bioavailability, and Internal Handling: Mercury-Phytoplankton Interactions. *Environmental Toxicology and Chemistry* **2014**, *33* (6), 1211–1224. <https://doi.org/10.1002/etc.2424>.
- (15) Pedrero, Z.; Bridou, R.; Mounicou, S.; Guyoneaud, R.; Monperrus, M.; Amouroux, D. Transformation, Localization, and Biomolecular Binding of Hg Species at Subcellular Level in Methylating and Nonmethylating Sulfate-Reducing Bacteria. *Environmental Science & Technology* **2012**, *46* (21), 11744–11751. <https://doi.org/10.1021/es302412q>.
- (16) Krupp, E. M.; Milne, B. F.; Mestrot, A.; Meharg, A. A.; Feldmann, J. Investigation into Mercury Bound to Biothiols: Structural Identification Using ESI-Ion-Trap MS and Introduction of a Method for Their HPLC Separation with Simultaneous Detection by ICP-MS and ESI-MS. *Anal Bioanal Chem* **2008**, *390* (7), 1753–1764. <https://doi.org/10.1007/s00216-008-1927-x>.
- (17) Pedrero, Z.; Ouerdane, L.; Mounicou, S.; Lobinski, R.; Monperrus, M.; Amouroux, D. Identification of Mercury and Other Metals Complexes with Metallothioneins in Dolphin Liver by Hydrophilic Interaction Liquid Chromatography with the Parallel Detection by ICP MS and Electrospray Hybrid Linear/Orbital Trap MS/MS. *Metallomics* **2012**, *4* (5), 473. <https://doi.org/10.1039/c2mt00006g>.
- (18) Klein, M.; Ouerdane, L.; Bueno, M.; Pannier, F. Identification in Human Urine and Blood of a Novel Selenium Metabolite, Se-Methylselenoneine, a Potential Biomarker of Metabolization in Mammals of the Naturally Occurring Selenoneine, by HPLC Coupled to Electrospray Hybrid Linear Ion Trap-Orbital Ion Trap MS. *Metallomics* **2011**, *3* (5), 513. <https://doi.org/10.1039/c0mt00060d>.
- (19) Trümpler, S.; Lohmann, W.; Meermann, B.; Buscher, W.; Sperling, M.; Karst, U. Interaction of Thimerosal with Proteins—Ethylmercuryadduct Formation of Human Serum Albumin and β -Lactoglobulin A. *Metallomics* **2009**, *1* (1), 87–91. <https://doi.org/10.1039/B815978E>.

- (20) Mangal, V.; Phung, T.; Nguyen, T. Q.; Guéguen, C. Molecular Characterization of Mercury Binding Ligands Released by Freshwater Algae Grown at Three Photoperiods. *Front. Environ. Sci.* **2019**, *6*. <https://doi.org/10.3389/fenvs.2018.00155>.
- (21) Pedrero, Z.; Mounicou, S.; Monperrus, M.; Amouroux, D. Investigation of Hg Species Binding Biomolecules in Dolphin Liver Combining GC and LC-ICP-MS with Isotopic Tracers. *J. Anal. At. Spectrom.* **2011**, *26* (1), 187–194. <https://doi.org/10.1039/C0JA00154F>.
- (22) Pedrero Zayas, Z.; Ouerdane, L.; Mounicou, S.; Lobinski, R.; Monperrus, M.; Amouroux, D. Hemoglobin as a Major Binding Protein for Methylmercury in White-Sided Dolphin Liver. *Anal Bioanal Chem* **2014**, *406* (4), 1121–1129. <https://doi.org/10.1007/s00216-013-7274-6>.
- (23) Manceau, A.; Nagy, K. L.; Glatzel, P.; Bourdineaud, J.-P. Acute Toxicity of Divalent Mercury to Bacteria Explained by the Formation of Dicysteinate and Tetracysteinate Complexes Bound to Proteins in *Escherichia Coli* and *Bacillus Subtilis*. *Environ. Sci. Technol.* **2021**, *55* (6), 3612–3623. <https://doi.org/10.1021/acs.est.0c05202>.
- (24) Manceau, A.; Azemard, S.; Hédouin, L.; Vassileva, E.; Lecchini, D.; Fauvelot, C.; Swarzenski, P. W.; Glatzel, P.; Bustamante, P.; Metian, M. Chemical Forms of Mercury in Blue Marlin Billfish: Implications for Human Exposure. *Environ. Sci. Technol. Lett.* **2021**, *8* (5), 405–411. <https://doi.org/10.1021/acs.estlett.1c00217>.
- (25) Manceau, A.; Gaillot, A.-C.; Glatzel, P.; Cherel, Y.; Bustamante, P. In Vivo Formation of HgSe Nanoparticles and Hg–Tetraselenolate Complex from Methylmercury in Seabirds—Implications for the Hg–Se Antagonism. *Environ. Sci. Technol.* **2021**, *55* (3), 1515–1526. <https://doi.org/10.1021/acs.est.0c06269>.
- (26) Song, Y.; Adediran, G. A.; Jiang, T.; Hayama, S.; Björn, E.; Skjellberg, U. Toward an Internally Consistent Model for Hg(II) Chemical Speciation Calculations in Bacterium–Natural Organic Matter–Low Molecular Mass Thiol Systems. *Environ. Sci. Technol.* **2020**, *54* (13), 8094–8103. <https://doi.org/10.1021/acs.est.0c01751>.
- (27) Song, Y.; Jiang, T.; Liem-Nguyen, V.; Sparrman, T.; Björn, E.; Skjellberg, U. Thermodynamics of Hg(II) Bonding to Thiol Groups in Suwannee River Natural Organic Matter Resolved by Competitive Ligand Exchange, Hg L_{III}-Edge EXAFS and ¹H NMR Spectroscopy. *Environ. Sci. Technol.* **2018**, *52* (15), 8292–8301. <https://doi.org/10.1021/acs.est.8b00919>.
- (28) Liberton, M.; Page, L. E.; O'Dell, W. B.; O'Neill, H.; Mamontov, E.; Urban, V. S.; Pakrasi, H. B. Organization and Flexibility of Cyanobacterial Thylakoid Membranes Examined by Neutron Scattering. *J. Biol. Chem.* **2013**, *288* (5), 3632–3640. <https://doi.org/10.1074/jbc.M112.416933>.
- (29) Sarma, T. A. *Handbook of Cyanobacteria*, 0 ed.; CRC Press, 2012. <https://doi.org/10.1201/b14316>.
- (30) Stanier, R. Y.; Deruelles, J.; Rippka, R.; Herdman, M.; Waterbury, J. B. Generic Assignments, Strain Histories and Properties of Pure Cultures of Cyanobacteria. *Journal of General Microbiology* **1979**, *111* (1), 1–61. <https://doi.org/10.1099/00221287-111-1-1>.
- (31) Jaishankar, J.; Srivastava, P. Molecular Basis of Stationary Phase Survival and Applications. *Front. Microbiol.* **2017**, *8*, 2000. <https://doi.org/10.3389/fmicb.2017.02000>.
- (32) Muthusamy, S.; Lundin, D.; Branca, R. M. M.; Baltar, F.; González, J. M.; Lehtiö, J.; Pinhassi, J. Comparative Proteomics Reveals Signature Metabolisms of Exponentially Growing and Stationary Phase Marine Bacteria. *Environmental Microbiology* **2017**, *19* (6), 2301–2319. <https://doi.org/10.1111/1462-2920.13725>.

- (33) Lavoie, M.; Le Faucheur, S.; Fortin, C.; Campbell, P. G. C. Cadmium Detoxification Strategies in Two Phytoplankton Species: Metal Binding by Newly Synthesized Thiolated Peptides and Metal Sequestration in Granules. *Aquatic Toxicology* **2009**, *92* (2), 65–75. <https://doi.org/10.1016/j.aquatox.2008.12.007>.
- (34) Bridou, R.; Monperrus, M.; Gonzalez, P. R.; Guyoneaud, R.; Amouroux, D. Simultaneous Determination of Mercury Methylation and Demethylation Capacities of Various Sulfate-Reducing Bacteria Using Species-Specific Isotopic Tracers. *Environmental Toxicology and Chemistry* **2011**, *30* (2), 337–344. <https://doi.org/10.1002/etc.395>.
- (35) Schuurmans, R. M.; Matthijs, J. C. P.; Hellingwerf, K. J. Transition from Exponential to Linear Photoautotrophic Growth Changes the Physiology of *Synechocystis* Sp. PCC 6803. *Photosynth Res* **2017**, *132* (1), 69–82. <https://doi.org/10.1007/s11120-016-0329-8>.
- (36) Wu, Y.; Wang, W.-X. Thiol Compounds Induction Kinetics in Marine Phytoplankton during and after Mercury Exposure. *Journal of Hazardous Materials* **2012**, *217–218*, 271–278. <https://doi.org/10.1016/j.jhazmat.2012.03.024>.
- (37) Morelli, E.; Ferrara, R.; Bellini, B.; Dini, F.; Di Giuseppe, G.; Fantozzi, L. Changes in the Non-Protein Thiol Pool and Production of Dissolved Gaseous Mercury in the Marine Diatom *Thalassiosira weissflogii* under Mercury Exposure. *Science of The Total Environment* **2009**, *408* (2), 286–293. <https://doi.org/10.1016/j.scitotenv.2009.09.047>.
- (38) Wu, Y.; Wang, W.-X. Accumulation, Subcellular Distribution and Toxicity of Inorganic Mercury and Methylmercury in Marine Phytoplankton. *Environmental Pollution* **2011**, *159* (10), 3097–3105. <https://doi.org/10.1016/j.envpol.2011.04.012>.
- (39) Bravo, A. G.; Le Faucheur, S.; Monperrus, M.; Amouroux, D.; Slaveykova, V. I. Species-Specific Isotope Tracers to Study the Accumulation and Biotransformation of Mixtures of Inorganic and Methyl Mercury by the Microalga *Chlamydomonas Reinhardtii*. *Environmental Pollution* **2014**, *192*, 212–215. <https://doi.org/10.1016/j.envpol.2014.05.013>.
- (40) Wu, Y.; Wang, W.-X. Intracellular Speciation and Transformation of Inorganic Mercury in Marine Phytoplankton. *Aquatic Toxicology* **2014**, *148*, 122–129. <https://doi.org/10.1016/j.aquatox.2014.01.005>.
- (41) Pickhardt, P. C.; Fisher, N. S. Accumulation of Inorganic and Methylmercury by Freshwater Phytoplankton in Two Contrasting Water Bodies. *Environ. Sci. Technol.* **2007**, *41* (1), 125–131. <https://doi.org/10.1021/es060966w>.
- (42) Pickhardt, P. C.; Folt, C. L.; Chen, C. Y.; Klaue, B.; Blum, J. D. Impacts of Zooplankton Composition and Algal Enrichment on the Accumulation of Mercury in an Experimental Freshwater Food Web. *Science of The Total Environment* **2005**, *339* (1–3), 89–101. <https://doi.org/10.1016/j.scitotenv.2004.07.025>.
- (43) Elbaz, A.; Wei, Y. Y.; Meng, Q.; Zheng, Q.; Yang, Z. M. Mercury-Induced Oxidative Stress and Impact on Antioxidant Enzymes in *Chlamydomonas Reinhardtii*. *Ecotoxicology* **2010**, *19* (7), 1285–1293. <https://doi.org/10.1007/s10646-010-0514-z>.
- (44) Slaveykova, V. I.; Majumdar, S.; Regier, N.; Li, W.; Keller, A. A. Metabolomic Responses of Green Alga *Chlamydomonas Reinhardtii* Exposed to Sublethal Concentrations of Inorganic and Methylmercury. *Environ. Sci. Technol.* **2021**, *acs.est.0c08416*. <https://doi.org/10.1021/acs.est.0c08416>.
- (45) Devars, S.; Avilés, C.; Cervantes, C.; Moreno-Sánchez, R. Mercury Uptake and Removal by *Euglena Gracilis*. *Archives of Microbiology* **2000**, *174* (3), 175–180. <https://doi.org/10.1007/s002030000193>.

- (46) Narainsamy, K.; Farci, S.; Braun, E.; Junot, C.; Cassier-Chauvat, C.; Chauvat, F. Oxidative-Stress Detoxification and Signalling in Cyanobacteria: The Crucial Glutathione Synthesis Pathway Supports the Production of Ergothioneine and Ophthamate: Ophthamate an Evolutionary-Conserved Stress Marker. *Molecular Microbiology* **2016**, *100* (1), 15–24. <https://doi.org/10.1111/mmi.13296>.
- (47) Narainsamy, K.; Marteyn, B.; Sakr, S.; Cassier-Chauvat, C.; Chauvat, F. Genomics of the Pleiotropic Glutathione System in Cyanobacteria. In *Advances in Botanical Research*; Elsevier, 2013; Vol. 65, pp 157–188. <https://doi.org/10.1016/B978-0-12-394313-2.00005-6>.
- (48) Bellini, E.; Varotto, C.; Borsò, M.; Rugnini, L.; Bruno, L.; Sanità di Toppi, L. Eukaryotic and Prokaryotic Phytochelatin Synthases Differ Less in Functional Terms Than Previously Thought: A Comparative Analysis of Marchantia Polymorpha and Geitlerinema Sp. PCC 7407. *Plants* **2020**, *9* (7), 914. <https://doi.org/10.3390/plants9070914>.
- (49) Kelly, D. J. A.; Budd, K.; Lefebvre, D. D. The Biotransformation of Mercury in PH-Stat Cultures of Microfungi. *Canadian Journal of Botany* **2006**, *84* (2), 254–260. <https://doi.org/10.1139/b05-156>.
- (50) Jones, G. J.; Palenik, B. P.; Morel, F. M. M. TRACE METAL REDUCTION BY PHYTOPLANKTON: THE ROLE OF PLASMALEMMA REDOX ENZYMES. *J Phycol* **1987**, *23* (s2), 237–244. <https://doi.org/10.1111/j.1529-8817.1987.tb04131.x>.
- (51) Schaefer, J. K.; Morel, F. M. M. High Methylation Rates of Mercury Bound to Cysteine by *Geobacter Sulfurreducens*. *Nature Geoscience* **2009**, *2* (2), 123–126. <https://doi.org/10.1038/ngeo412>.
- (52) Schaefer, J. K.; Rocks, S. S.; Zheng, W.; Liang, L.; Gu, B.; Morel, F. M. M. Active Transport, Substrate Specificity, and Methylation of Hg(II) in Anaerobic Bacteria. *Proceedings of the National Academy of Sciences of the United States of America* **2011**, *108* (21), 8714–8719. <https://doi.org/10.1073/pnas.1105781108>.
- (53) Du, W.; Liu, Y.; Sun, J.; Wu, N.; Mai, Y.; Wang, C. The Aquatic Microbial Community: A Bibliometric Analysis of Global Research Trends (1991–2018). *fal* **2020**, *194* (1), 19–32. <https://doi.org/10.1127/fal/2020/1305>.
- (54) Basińska, A. M.; Reczuga, M. K.; Gąbka, M.; Stróżecki, M.; Łuców, D.; Samson, M.; Urbaniak, M.; Leśny, J.; Chojnicki, B. H.; Gilbert, D.; Sobczyński, T.; Olejnik, J.; Silvennoinen, H.; Juszczak, R.; Lamentowicz, M. Experimental Warming and Precipitation Reduction Affect the Biomass of Microbial Communities in a Sphagnum Peatland. *Ecological Indicators* **2020**, *112*, 106059. <https://doi.org/10.1016/j.ecolind.2019.106059>.
- (55) Lürling, M.; Eshetu, F.; Faassen, E. J.; Kosten, S.; Huszar, V. L. M. Comparison of Cyanobacterial and Green Algal Growth Rates at Different Temperatures: *Temperature and Phytoplankton Growth Rates*. *Freshwater Biology* **2013**, *58* (3), 552–559. <https://doi.org/10.1111/j.1365-2427.2012.02866.x>.
- (56) Ji, M.; Liu, Z.; Sun, K.; Li, Z.; Fan, X.; Li, Q. Bacteriophages in Water Pollution Control: Advantages and Limitations. *Front. Environ. Sci. Eng.* **2021**, *15* (5), 84. <https://doi.org/10.1007/s11783-020-1378-y>.

Supporting Information

Determination of the intracellular complexation of inorganic and methylmercury in cyanobacterium *Synechocystis* sp. PCC 6803

Javier Garcia-Calleja¹, Thibaut Cossart², Zoyne Pedrero¹, João P. Santos², Laurent Ouerdane¹, Emmanuel Tessier¹, Vera I. Slaveykova², David Amouroux¹

¹ Université de Pau et des Pays de l'Adour, E2S UPPA, CNRS, IPREM, Institut des Sciences Analytiques et de Physico-chimie pour l'Environnement et les matériaux, Pau, France,

² University of Geneva, Faculty of Sciences, Earth and Environment Sciences, Department F.-A. Forel for Environmental and Aquatic Sciences, Uni Carl Vogt, 66 Bvd. Carl Vogt, CH-1211 Geneva, Switzerland

Corresponding Authors:

Javier Garcia-Calleja E-mail: javier.garcia-calleja@univ-pau.fr (J.C) phone: +34 669159412

Zoyne Pedrero E-mail: zoyne.prederozayas@univ-pau.fr (Z.P) phone: +33 540175027

LIST OF FIGURES

Figure S1. Hg control contamination in the intracellular fraction.

Figure S2. Scheme of the cell fractionation procedure.

Figure S3. Match standard glutathione in peptide column.

Figure S4. Conceptual scheme of the isotopic pattern deconvolution methodology for the determination of ^{199}iHg and Me^{201}Hg by using another two analytical spikes (^{198}iHg and Me^{202}Hg).

Figure S5. SEC profiles of essential trace metals.

Figure S6. Parallel detection by HILIC-ICP-MS and HILIC-ESI-MS.

LIST OF TABLES

Table S1. Growth medium composition (BG11 medium).

Table S2. Operating parameters for SEC-ICP-MS and HILIC-ESI-MS analysis.

Table S3. Operating parameters GC-ICP-MS.

Table S1. Growth medium composition (BG11 medium).

Composition	Concentration (g L ⁻¹)
H₃BO₃	2.9
MnCl₂.4H₂O	1.8
ZnSO₄. 7H₂O	0.2
Na₂MoBO₄.2H₂O	0.4
CuSO₄.5H₂O	0.079
Co(NO₃)₂.6H₂O	49.4
K₂HPO₄	4.0
MgSO₄.7H₂O	7.5
CaCl₂.2H₂O	3.6
Citric acid (C₆H₈O₇)	6.0
Na₂EDTA.2H₂O	0.1
Ferric ammonium citrate (C₆H₈FeNO₇)	6.0
Na₂CO₃	2.0

Exposure medium composition: Same composition as growth medium except for the trace elements stock solution, acids and EDTA.

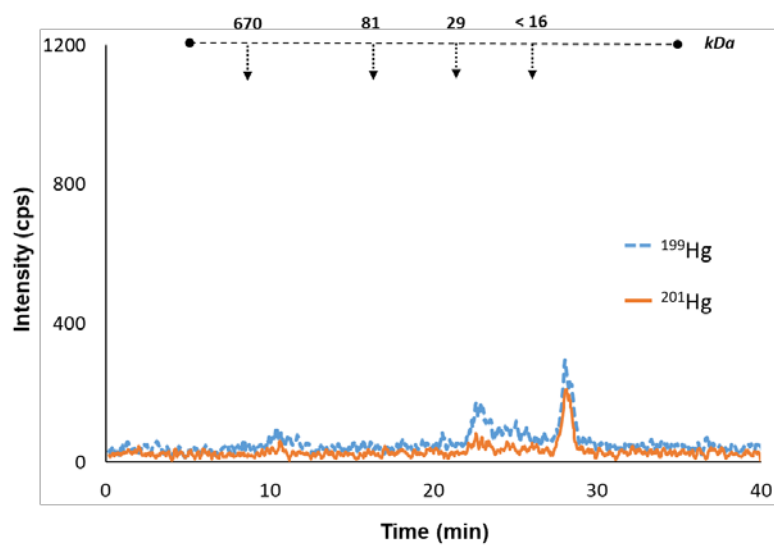


Figure S1. Size exclusion chromatograms (Range: 600-10 kDa) in the intracellular compartment of *Synechocystis* sp. PCC 6803 by ICP-MS detection ^{199}Hg and ^{201}Hg corresponding to the control (no Hg addition).

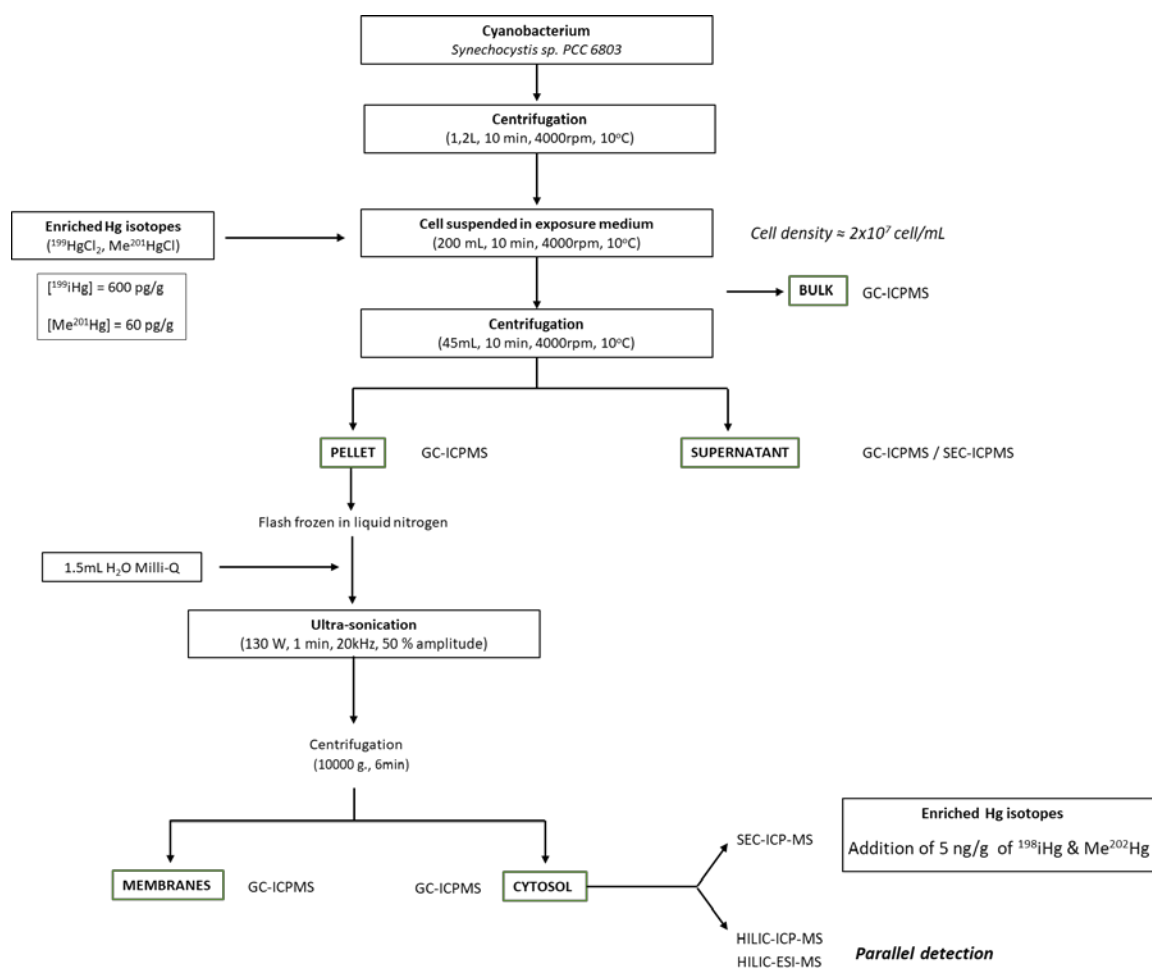


Figure S2. Scheme of the cell fractionation procedure used to obtain the bulk and cytosolic fraction. **GC-ICP-MS** was used for Hg species quantification and **SEC/HILIC-ICP-MS and HILIC-ESI-MS** was used for the investigation of Hg binding biomolecules. All measurements were done in triplicate.

Table S2. Operating parameters for Size Exclusion Chromatography and Hydrophilic Interaction Liquid Chromatography coupled to ICP-MS and ESI-MS analysis.

Parameters	SEC	HILIC
Type of column	Superdex TM 200 Increase 10/300 GL (10x300)	TSK gel amide 80 column (250 mm×1 mm i.d., 5 µm)
Mobile phase	A: 100 mM Ammonium Acetate H ₂ O Milli-Q pH:7.4	A: ACN B: 10 mM Ammonium Formate pH:5
Mode	Isocratic	Gradient ¹
Flow rate	100 mL/min	50 µL/min
Range	600-10 kDa	Polar biomolecules separation
Injection volume	100 µL	7 µL
Ionization source	ICP	ICP / ESI
Mass analyzer	Quadrupole	Quadrupole/ Orbitrap

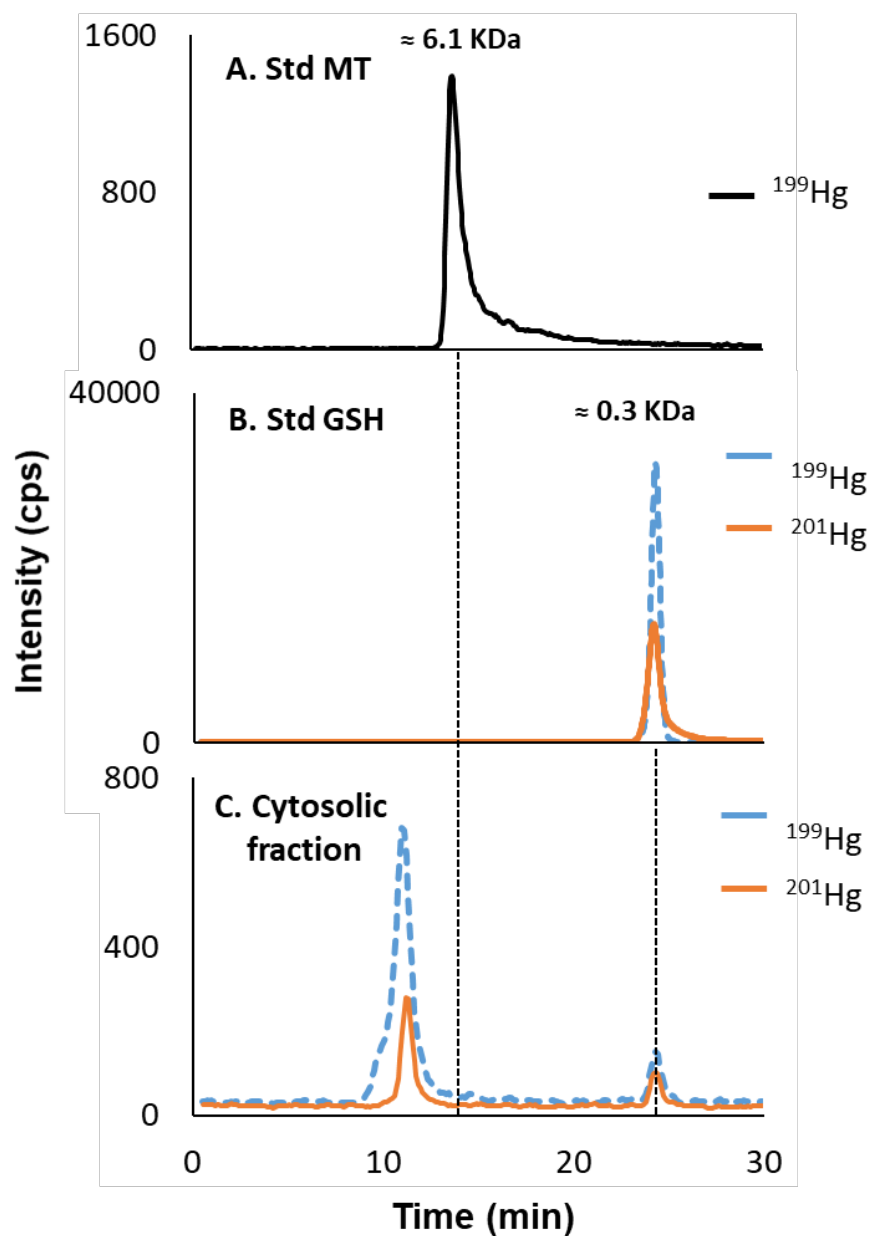


Figure S3. Size exclusion chromatograms (Range: 7- 0.1 kDa) by ICP-MS detection of (A) standard of metallothionein (MT) binding ^{199}iHg . (B) standard of Glutathione (GSH) binding ^{199}iHg and Me^{201}Hg . (C) the cytosolic fraction of *Synechocystis* sp. PCC 6803 corresponding to both Hg isotopic tracers (^{199}iHg and Me^{201}Hg) after 24 hours of exposure.

Table S3. Operating parameters for Gas Chromatography coupled to Inductively Coupled Plasma Mass Spectrometry analysis for Hg species quantification.

Parameters	GC-ICPMS
Type of column	R x 1-5ms Crossbond 5% diphenyl/ 95% polysiloxane (30m x 0.25mm x 0.25µm)
Injector Mode	Splitless
Injector Temperature	250 °C
Interphase Temperature	280 °C
Injection volume	2 µL
Carrier flow rate	5mL/min (He)
Acquisition mode	Transient Time Resolved Analysis
Acquisition Time	300 sec.
Dwell Time	20 ms
Isotopes measured	¹⁹⁶ Hg, ¹⁹⁸ Hg, ¹⁹⁹ Hg, ²⁰⁰ Hg, ²⁰¹ Hg, ²⁰² Hg, ²⁰⁴ Hg, ²⁰³ Tl, ²⁰⁵ Tl

Mathematical approach: quantification of the cytosolic fraction by double species-specific isotopic dilution analysis.

Data treatment. For the determination of the concentration of both Hg isotopic tracers, it was assumed that the isotopic composition in a mixture of natural abundance and four Hg labelled, both for inorganic mercury and methyl mercury, was a linear combination of the isotopes patterns of the different constituents of the mixture (culture enriched spikes in ^{199}iHg and Me^{201}Hg , quantification enriched spikes with ^{198}iHg and Me^{202}Hg and mercury natural abundance). The general equations for the double species-specific isotopic dilution analysis are based on isotope pattern deconvolution². Expressing the Hg natural isotope abundance, isotope abundances of the Hg culture enriched tracers (^{199}iHg and Me^{201}Hg) and isotope abundances of the Hg enriched spikes for the quantification (^{198}iHg and Me^{202}Hg), we can calculate the five molar fractions resolving a multiple linear regression (Figure S3).

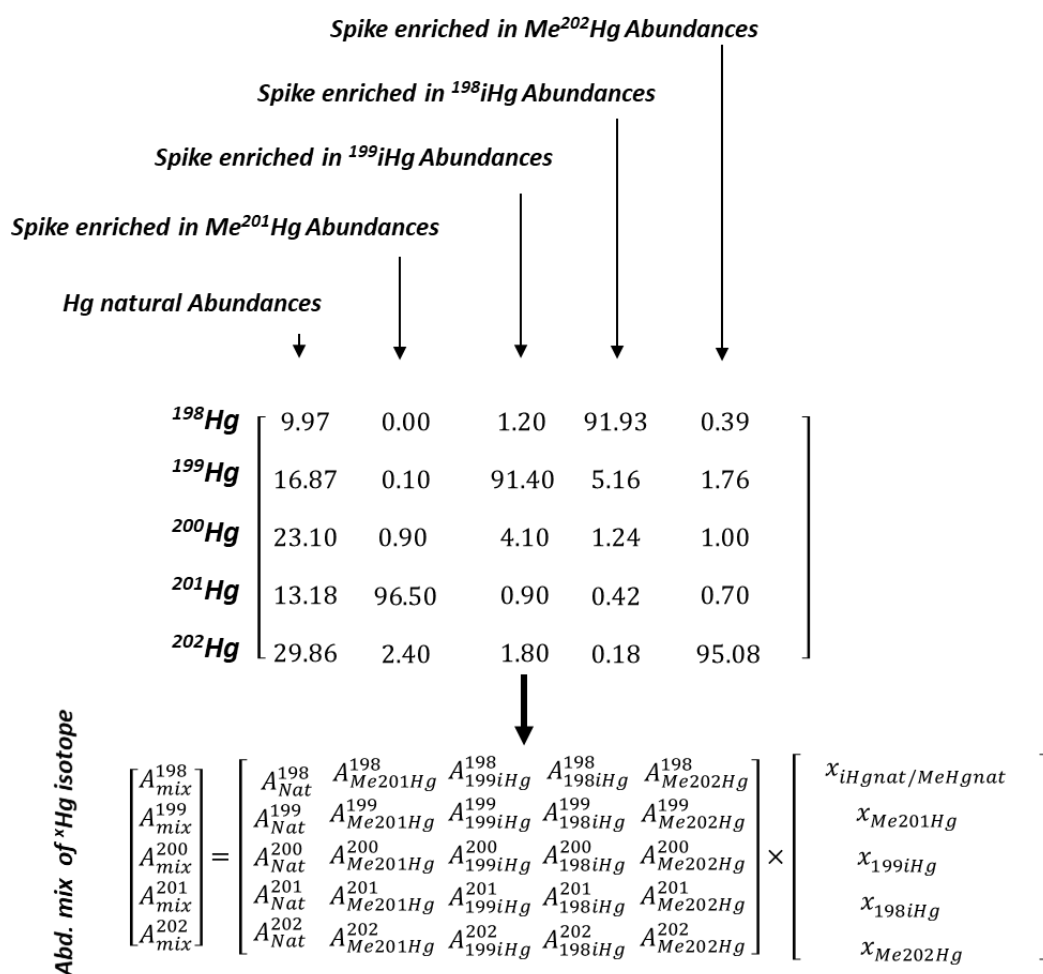


Figure S4. Conceptual scheme of the isotopic pattern deconvolution methodology for the determination of ¹⁹⁹iHg and Me²⁰¹Hg using another two analytical enriched Hg isotopes (¹⁹⁸iHg and Me²⁰²Hg).

Then, we can calculate the concentrations of different analogues from their molar fractions. In our system, the number isotopes measured comprise the same number of Hg isotopes sources. Theoretically, we should have a mixture of four Hg labelled species before the analysis. Nevertheless, this procedure allows controlling any possible contamination coming from natural Hg (natural isotopic abundance), but even more relevant, it allows to determine both Hg species concentrations and transformation (methylation and demethylation) affecting the two isotopic tracers during the analytical procedure. More details on the mathematical approach are explained elsewhere^{3,4}.

S5. SEC profiles essential trace metals.

○ Cobalt (A)

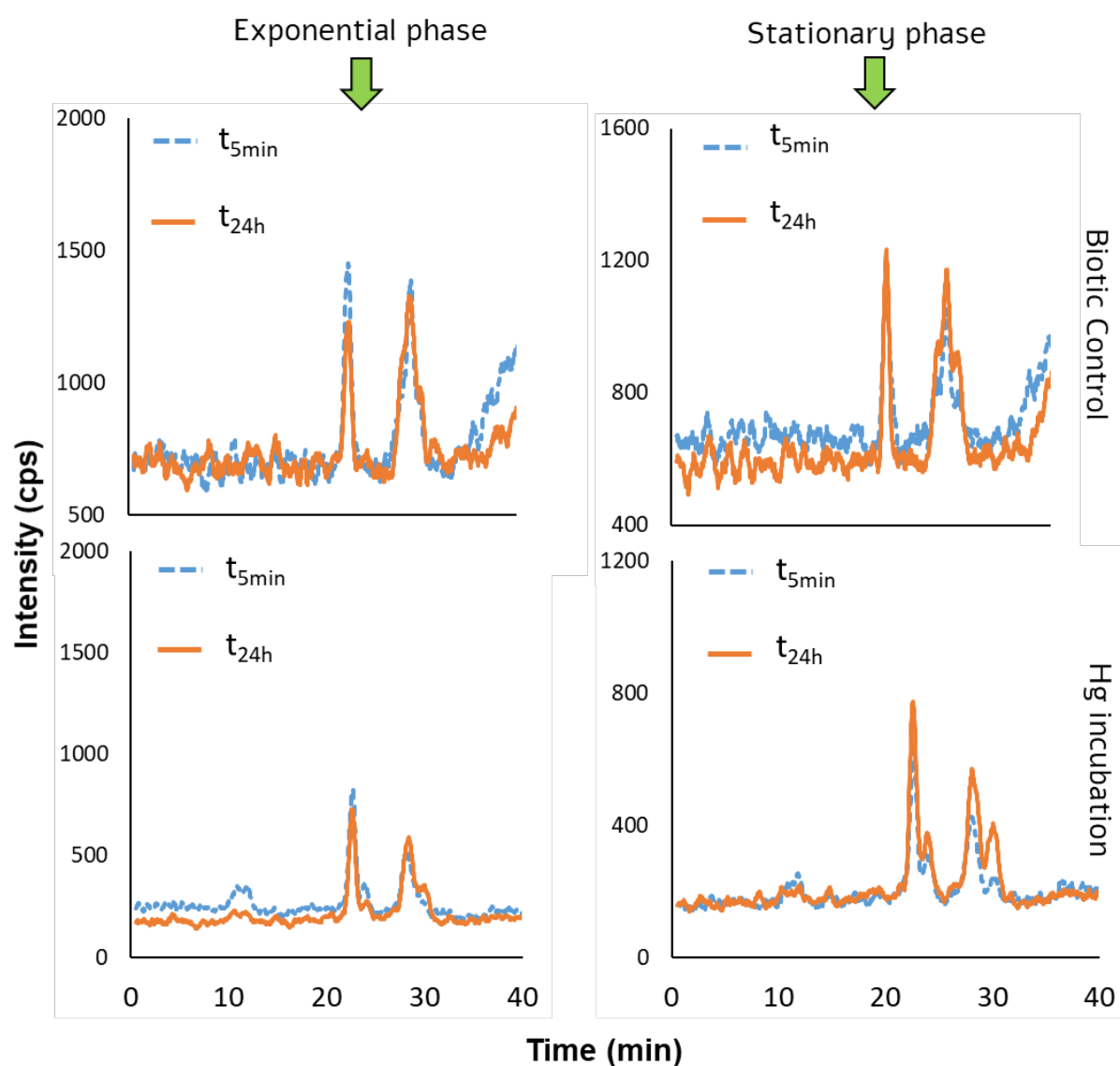


Figure S5A. Size exclusion chromatograms Superdex 200 (Range: 600 - 10 kDa) in the intracellular compartment of *Synechocystis* sp. PCC 6803 by ICP-MS detection of ^{59}Co corresponding to the biotic control and Hg incubation experiment in the exponential and stationary phase after 5 minutes and 24 hours.

○ **Iron (B)**

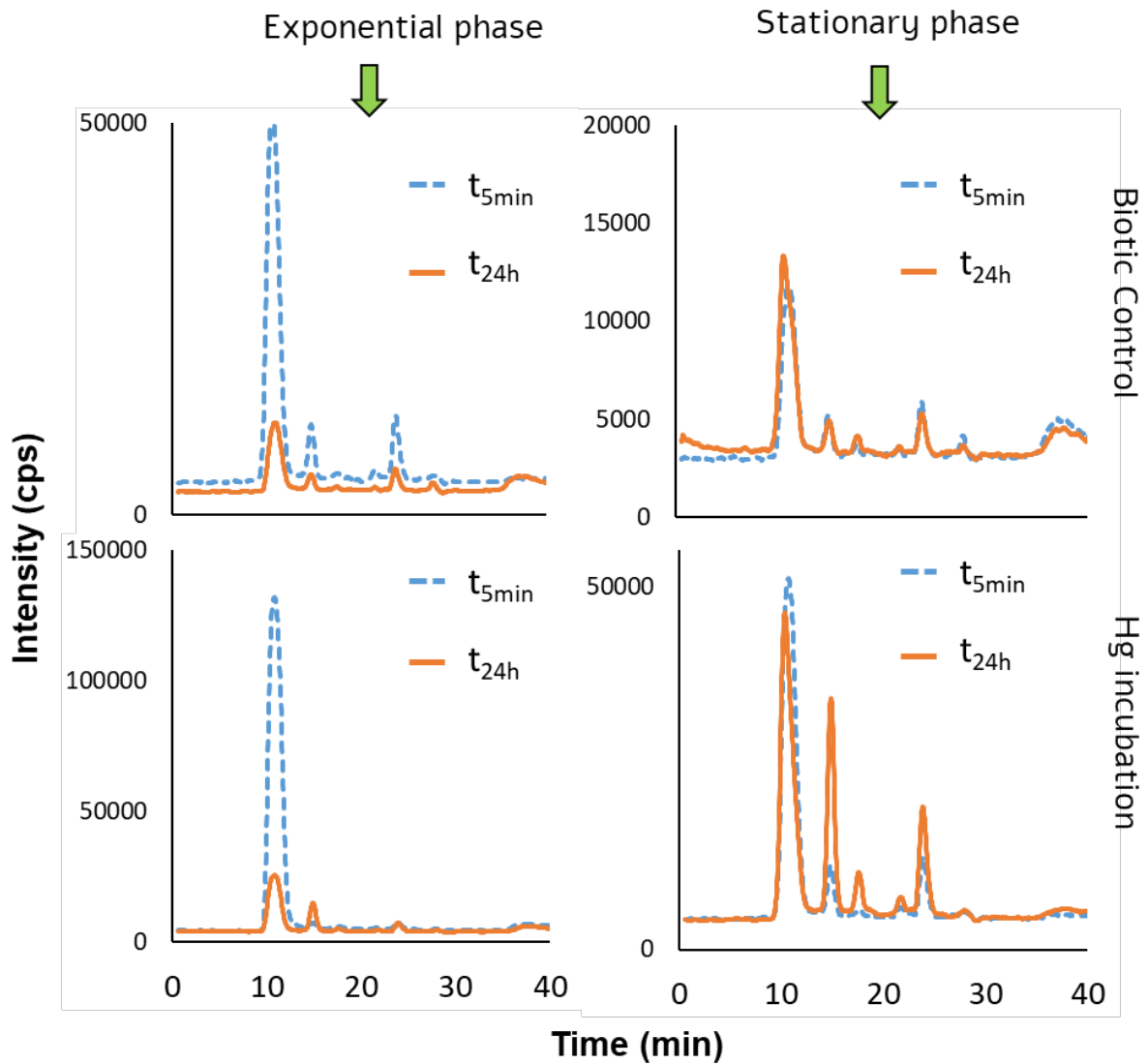


Figure S5B. Size exclusion chromatograms Superdex 200 (Range: 600 - 10 kDa) in the intracellular compartment of *Synechocystis* sp. PCC 6803 by ICP-MS detection of ^{57}Fe corresponding to the biotic control and Hg incubation experiment in the exponential and stationary phase after 5 minutes and 24 hours.

○ **Copper (C)**

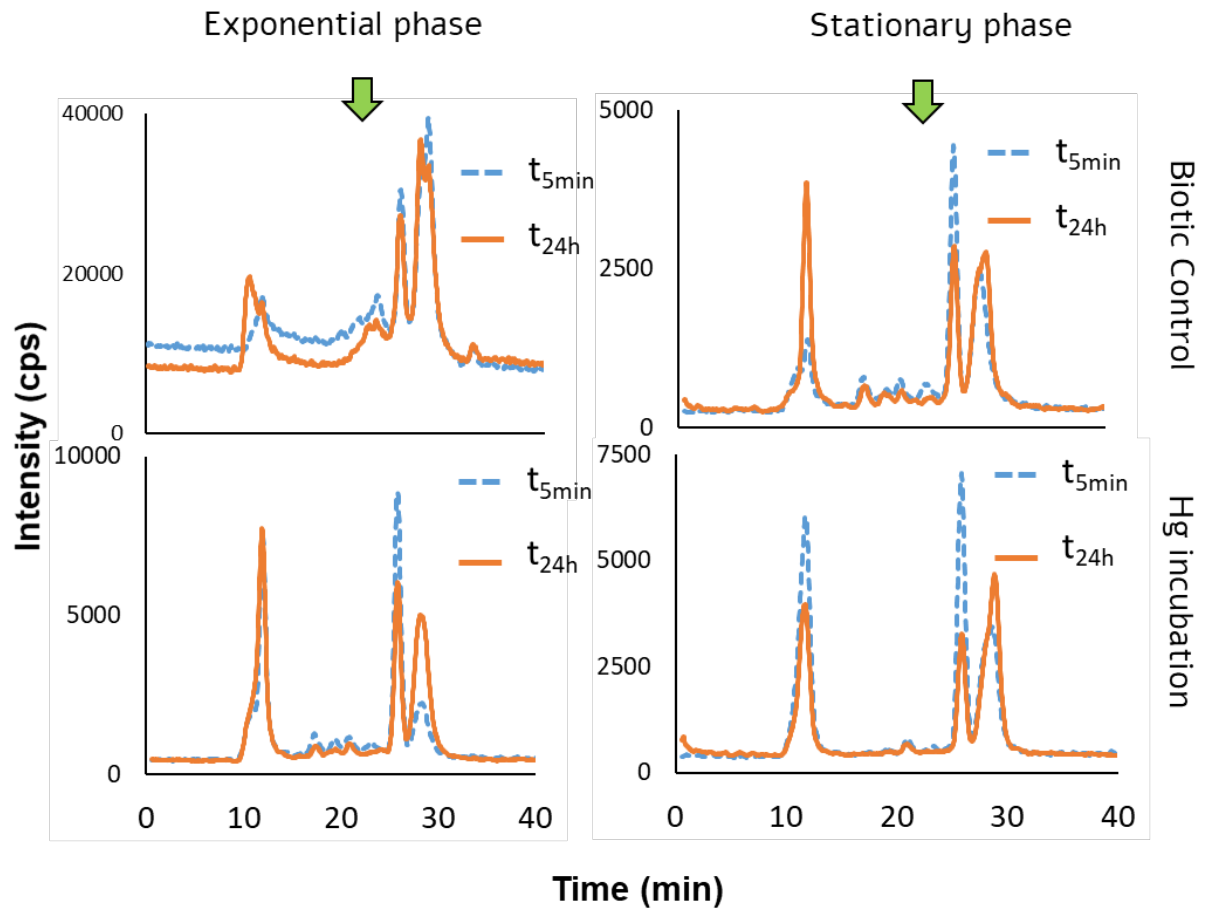


Figure S5C. Size exclusion chromatograms Superdex 200 (Range: 600 - 10 kDa) in the intracellular compartment of *Synechocystis* sp. PCC 6803 by ICP-MS detection of ^{63}Cu corresponding to the biotic control and Hg incubation experiment in the exponential and stationary phase after 5 minutes and 24 hours.

○ **Zinc (D)**

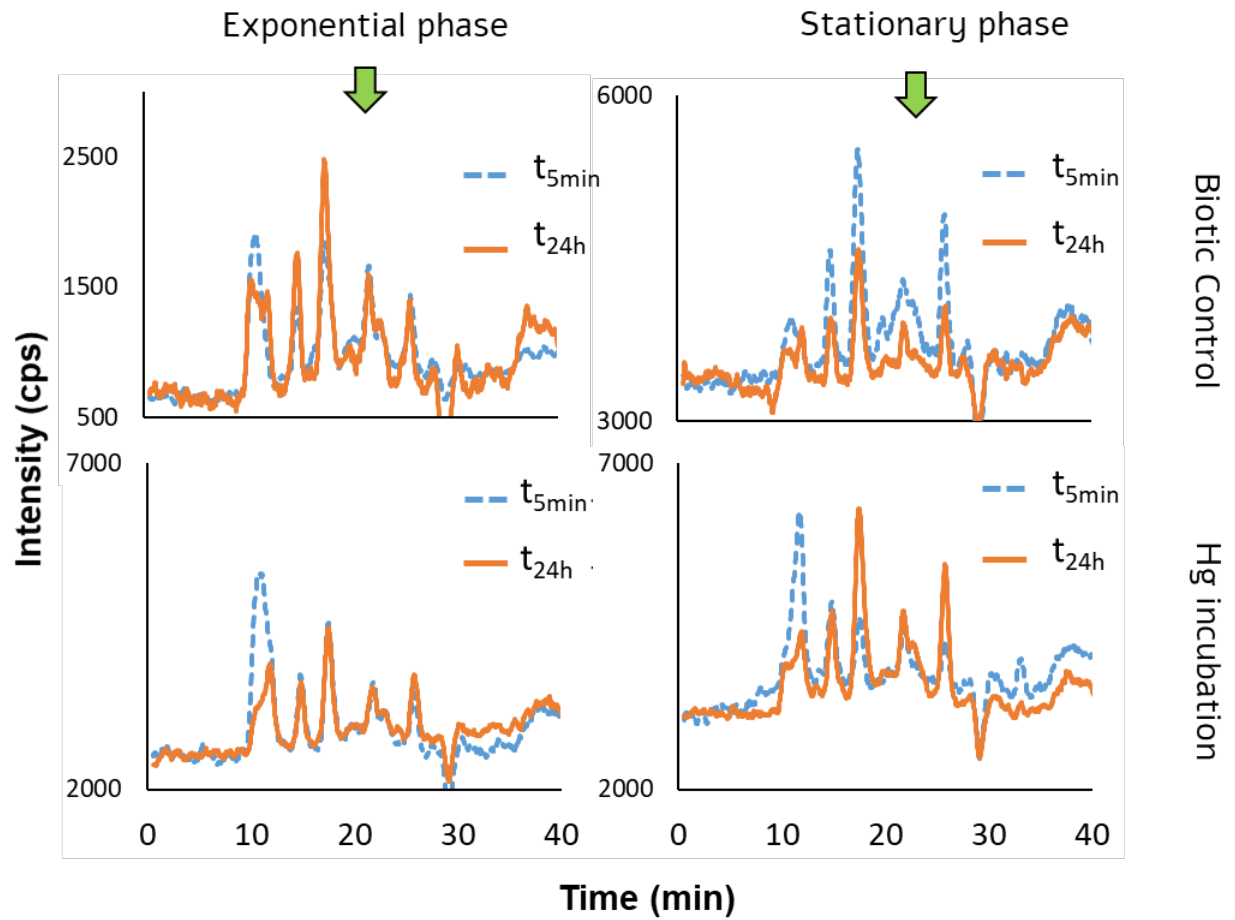


Figure S5D. Size exclusion chromatograms Superdex 200 (Range: 600 - 10 kDa) in the intracellular compartment of *Synechocystis* sp. PCC 6803 by ICP-MS detection of ^{66}Zn corresponding to the biotic control and Hg incubation experiment in the exponential and stationary phase after 5 minutes and 24 hours.

S6. Parallel detection by HILIC-ICP-MS and HILIC-ESI-MS.

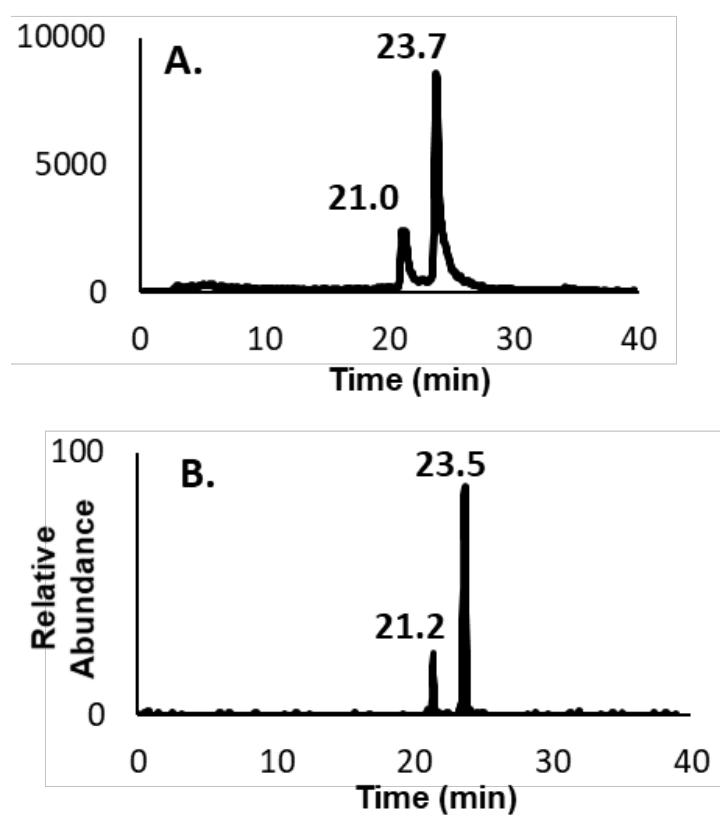


Figure S6. HILIC chromatogram of the cytosolic fraction by (A) ICP-MS detection of ^{202}Hg and (B) ESI-LTQ Orbitrap MS detection.

References.

- (1) Klein, M.; Ouerdane, L.; Bueno, M.; Pannier, F. Identification in Human Urine and Blood of a Novel Selenium Metabolite, Se-Methylselenoneine, a Potential Biomarker of Metabolization in Mammals of the Naturally Occurring Selenoneine, by HPLC Coupled to Electrospray Hybrid Linear Ion Trap-Orbital Ion Trap MS. *Metallomics* **2011**, 3 (5), 513. <https://doi.org/10.1039/c0mt00060d>.
- (2) Rodriguez-Gonzalez, P.; Bouchet, S.; Monperrus, M.; Tessier, E.; Amouroux, D. In Situ Experiments for Element Species-Specific Environmental Reactivity of Tin and Mercury Compounds Using Isotopic Tracers and Multiple Linear Regression. *Environ. Sci. Pollut. Res.* **2013**, 20 (3), 1269–1280. <https://doi.org/10.1007/s11356-012-1019-5>.
- (3) Rodríguez-González, P.; Monperrus, M.; García Alonso, J. I.; Amouroux, D.; Donard, O. F. X. Comparison of Different Numerical Approaches for Multiple Spiking Species-Specific Isotope Dilution Analysis Exemplified by the Determination of Butyltin Species in Sediments. *J. Anal. At. Spectrom.* **2007**, 22 (11), 1373. <https://doi.org/10.1039/b706542f>.
- (4) Monperrus, M.; Krupp, E.; Amouroux, D.; Donard, O. F. X.; Rodríguez Martín-Doimeadios, R. C. Potential and Limits of Speciated Isotope-Dilution Analysis for Metrology and Assessing Environmental Reactivity. *TrAC Trends Anal. Chem.* **2004**, 23 (3), 261–272. [https://doi.org/10.1016/S0165-9936\(04\)00313-9](https://doi.org/10.1016/S0165-9936(04)00313-9).